



Molecular modeling study on the effect of residues distant from the nucleotide-binding portion on RNA binding in *Staphylococcus aureus* Hfq

Prettina Lazar^a, Songmi Kim^a, Yuno Lee^a, Minky Son^a, Hyong-Ha Kim^b,
Yong Seong Kim^c, Keun Woo Lee^{a,*}

^a Division of Applied Life Science (BK21 Program), Environmental Biotechnology National Core Research Center (EB-NCRC), Plant Molecular Biology and Biotechnology Research Center (PMBBRC), Gyeongsang National University (GNU), Jinju 660-701, Republic of Korea

^b Division of Quality of Life, Korea Research Institute of Standards and Science, Daejeon 305-340, Republic of Korea

^c Department of Science Education, Kyungnam University, Masan 631-701, Republic of Korea

ARTICLE INFO

Article history:

Received 22 April 2009

Received in revised form 20 July 2009

Accepted 3 August 2009

Available online 8 August 2009

Keywords:

Hfq

RNA-binding bacterial protein

Nucleotide binding portion (NBP)

Molecular dynamics (MDs) simulation

Point mutation

RNA pore diameter

Destabilization

RNA–protein complex

ABSTRACT

Hfq is an abundant RNA-binding bacterial protein that was first identified in *E. coli* as a required host factor for phage Q β RNA replication. The pleiotropic phenotype resulting from the deletion of Hfq predicates the importance of this protein. Two RNA-binding sites have been characterized: the proximal site which binds sRNA and mRNA and the distal site which binds poly(A) tails. Previous studies mainly focused on the key residues in the proximal site of the protein. A recent mutation study in *E. coli* Hfq showed that a distal residue Val43 is important for the protein function. Interestingly, when we analyzed the sequence and structure of *Staphylococcus aureus* Hfq using the CONSEQ server, the results elicited that more functional residues were located far from the nucleotide-binding portion (NBP). From the analysis seven individual residues Asp9, Leu12, Glu13, Lys16, Gln31, Gly34 and Asp40 were selected to investigate the conformational changes in Hfq–RNA complex due to point mutation effect of those residues using molecular dynamics simulations. Results showed a significant effect on Asn28 which is an already known highly conserved functionally important residue. Mutants D9A, E13A and K16A depicted effects on base stacking along with increase in RNA pore diameter, which is required for the threading of RNA through the pore for the post-translational modification. Further, the result of protein stability analysis by the CUPSAT server showed destabilizing effect in the most mutants. From this study we characterized a series of important residues located far from the NBP and provide some clues that those residues may affect sRNA binding in Hfq.

© 2009 Elsevier Inc. All rights reserved.

1. Introduction

Hfq is an abundant RNA-binding bacterial protein that was first identified as a host factor required for replication of Q β RNA bacteriophage [1]. In bacterial cells, Hfq appears to function as a global regulator of gene expression. The pleiotropic phenotype resulting from the deletion of Hfq predicates the importance of this protein. The RNA-binding protein Hfq is involved in stress response and virulence of several Gram-negative pathogens [2–8] and Gram-positive pathogens [9], probably due to its roles as mediator in small RNA (sRNA)–mRNA and their mRNA targets [10,11]. Genome analysis shows that Hfq-like proteins are conserved in many (but not all) Gram-negative and Gram-positive bacteria [12].

Staphylococcus aureus is a Gram-positive pathogen responsible for a wide variety of human infections, ranging from superficial skin and wound infections to deep abscesses, septicemia, or toxin-associated syndromes [13]. The type of infection caused by *S. aureus* depends on virulence factors and stress response pathways present in infectious strains, and reflects the coordinated action of numerous regulators [14]. *S. aureus* encodes one Hfq-like protein whose structure has been already described with a molecular weight of 8.9 kDa. It is speculated that the Hfq protein is probably less abundant in *S. aureus* than in *E. coli*. Currently the only available crystal structure for the Hfq–RNA bound form is the complex between *S. aureus* Hfq and the hepta-oligoribonucleotide, AU₅G and is available in the PDB databank having PDB ID:1KQ2, resolved at 2.71 Å. It has provided basic information on how RNA can interact with riboregulator. The structure shows a clear picture of the binding mechanism of adenosine and uridine-rich stretch with Hfq. The RNA expands and fills the proximal site, central pore region of the hexamer, and binds in a circular manner except for

* Corresponding author.

E-mail address: kwlee@gnu.ac.kr (K.W. Lee).

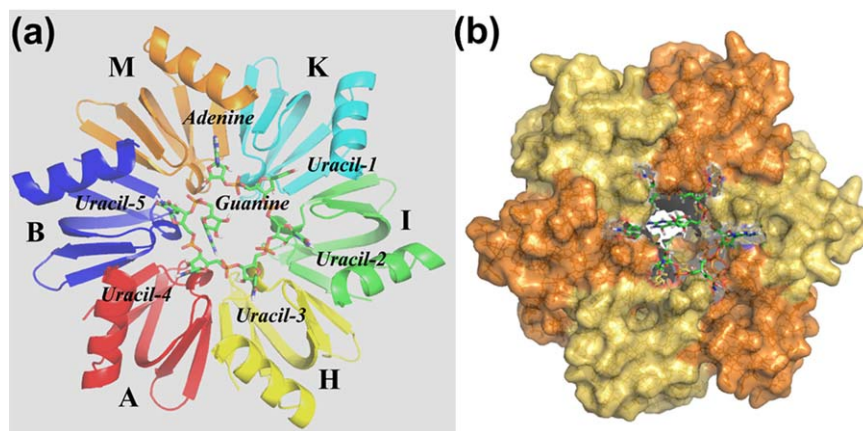


Fig. 1. Crystal structure arrangement details of *S. aureus* Hfq chains and bound RNA. (a) Secondary structure representation of Hfq, showing each chain in different colors and the bound RNA shown as stick model. (b) Shows the surface representation of the Hfq with the well-stacked RNA in stick model.

the 3'-guanosine, which is located at the entrance of the pore (Fig. 1). Each of the six potential AU nucleotide-binding pockets is composed of residues from two adjacent subunits. Both uridine and adenosine bind similarly, whereby their nucleobases stack against the aromatic side chain of residue Tyr42 and the same residue from a neighboring subunit [15].

One of the first connections between the ability of Hfq to bind small ncRNAs and its role in post-transcriptional regulation become evident in studies on OxyS. It is a 109 nucleotide regulator of the oxidative stress response. This sRNA was shown to bind directly to Hfq and thereby increase OxyS RNA interaction with *rpoS* mRNA as a part of its mechanism to inhibit *rpoS* translation [16,17]. Until now only two RNA-binding sites have been characterized in *E. coli*: proximal site which binds with sRNA and mRNA, and distal site which binds to poly(A) tails. Reports indicate that *S. aureus* Hfq does not bind to poly(A) with high affinity at the distal face of the pore comparing to the *E. coli* Hfq which has exceedingly high positive charge at the distal side [18].

A recent mutation study showed that in *E. coli* Hfq a distal residue Val43 plays an important role in the function of the protein. Several studies have aimed at identifying the key residues at the functional regions of Hfq [19]. When we analyzed the sequence and structure of the *S. aureus* Hfq protein by the CONSEQ server [20], it was interestingly found to have some structural and functional residues that were located far from the proximal part of the protein. Molecular dynamics (MDs) simulation study has been employed to examine the structurally and functionally important residues that are far from the nucleotide-binding portion (NBP) which may lead to the destabilization of the RNA–protein complex and hence the protein function and mechanism. We performed two 3 ns MD simulations of the Hfq protein with and without RNA to study the influence on conformation by the presence of RNA on the protein. The sequence of RNA used in the simulation is a hepta-oligoribonucleotide–5'-A-U-U-U-U-U-G-3' with the terminals capped. Also we performed seven individual 3 ns MD simulation runs of the Hfq–RNA complex, with each system having point mutation of one residue on each monomer at a time of the seven residues picked from the server analysis to study the importance of residues far from NBP using AMBER force field. Mutations were done to each monomer and hence the single mutant was really a hexamutant, which was employed for our study.

Overall, this study is aimed to unveil the role of the chosen distant residues in protein conformation and RNA binding through MD simulation and CONSEQ/CUPSAT analyses.

2. Methods

2.1. Sequence analysis by CONSEQ server

The CONSEQ program server (<http://conseq.bioinfo.tau.ac.il>) [20] was used to determine the highly conserved structurally and functionally important residues from the sequence reflected by means of the multiple sequence alignments of Hfq homolog proteins. This server compares the sequence of a reference protein with proteins deposited in Swiss-Prot in order to find homologs. The number of PSI-BLAST iterations and the *E* value cutoff used were 1 and 0.001, respectively. There were 256 PSI-BLAST hits obtained, 107 of them were unique sequences and the calculations were performed on the 50 homolog sequences with the lowest *E* value. All of the sequences that were found to be evolutionarily related with the Hfq proteins in the data set were used in conservation scoring. Briefly, the CONSEQ server assigns a conservation score to each residue taking into account the evolutionary relationships among the family of homologs. The scores are normalized as that the average score is zero, and negative and positive deviations represent the degrees of conservation and variation, respectively.

2.2. Molecular dynamics simulation

The GROMACS package [21,22] was used to perform MD simulations, while the protein and water molecules are described by parameters from AMBER99 [23] and TIP3P [24] force fields, respectively. Hydrogens were added and the protonation state of ionizable groups was chosen appropriate to pH 7.0. A solvent cubic box with length 12 nm was generated to perform the simulations in an aqueous environment. Six Na⁺ or Cl⁻ counter-ions were added by replacing water molecules to ensure the overall charge neutrality of the simulated system. The particle mesh Ewald (PME) method was applied to accurately determine the long-range electrostatic interactions [25]. A grid spacing of 1.2 Å for the fast Fourier transform calculation and VdW interactions were considered by applying a cutoff of 9 Å. A constant temperature and pressure for the whole system (300 K and 1 bar) are achieved with the Berendsen thermostat [26] and Parrinello and Rahman [27] barostat. The systems were subjected to a steepest descent energy minimization process until a tolerance of 1000 kJ/mol, step by step. The time step for the simulations was set to 2 fs. Then during the system equilibration process the protein backbone was frozen and the solvent molecules with counter-ions were allowed to move during a 50 ps position restrained MD run under NPT conditions at

Table 1
The system details for the molecular dynamics simulation study.

No.	System details	No. of TIP3P water added	No. of Cl ⁻ ion added	No. of Na ⁺ ions added
1	Hfq (apo)	20551	6	
2	Hfq + RNA	20494		
3	Hfq(D9A) + RNA	20514	6	–
4	Hfq(L12A) + RNA	20505	–	–
5	Hfq(E13A) + RNA	20525	6	
6	Hfq(K16A) + RNA	20507	–	6
7	Hfq(Q31A) + RNA	20504	–	–
8	Hfq(G34A) + RNA	20493	–	–
9	Hfq(D40A) + RNA	20541	6	–

300 K. The well equilibrated structure was then used for the 3 ns production runs. Bonds between heavy atoms and corresponding hydrogen atoms were constrained to their equilibrium bond lengths using the LINCS algorithm [28,29]. During the production

```

1      11      21      31
MIANENIQDK ALENFKANQT EVTVFFLNGF QMKGVIIEYD
e e e e e b e e b b e e e e e b b b b b b e e b e b e e e b e
f      f f      s f      f      f s      f s      f

41      51      61      71
KYVVSLSNSQG KQHLYIKHAI STYTVETEGQ ASTESEEE
e b b b b e e e e e e e e e b b b b b e e e e e e e e e e e e
                f f s      s s                        f f

```

Legend:

The conservation scale:



Variable Average Conserved

- e** - An exposed residue according to the neural-network algorithm.
- b** - A buried residue according to the neural-network algorithm.
- f** - A predicted functional residue (highly conserved and exposed).
- s** - A predicted structural residue (highly conserved and buried).

Fig. 2. CONSEQ server prediction of highly conserved exposed, buried, functional and structural residues, according to the neural-network algorithm for the *S. aureus* Hfq protein sequence is shown. Residue coloring is based on the conservation scale.

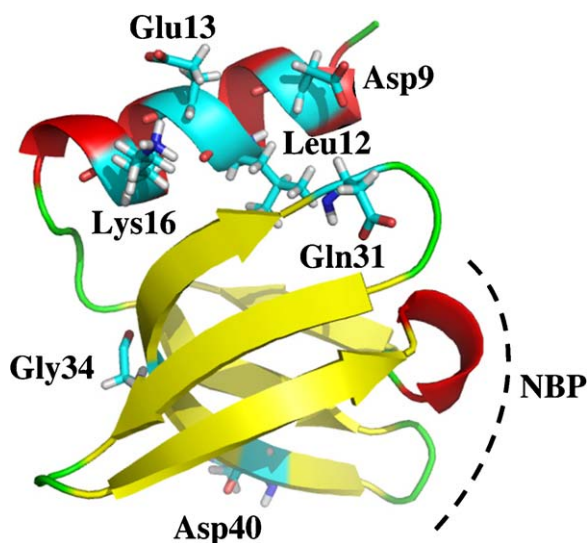


Fig. 3. Representation of monomer structure showing the location of the seven residues, Asp9, Leu12, Glu13, Lys16, Gln31, Gly34 and Asp40. Only a monomer structure was displayed in secondary structure format in order to clearly show the relative position of the residues from the nucleotide-binding portion (NBP).

phase, the coordinate data were written to the file every pico second (ps).

2.3. Simulation model system setup

A series of MD simulation calculations were carried out for the Hfq protein with and without bound RNA and also along with the seven mutants of D9A, L12A, E13A, K16A, Q31A, G34A and D40A that were considered on the Hfq hexamer (every single mutant was made on each monomer of the hexamer to form the hexamutant) based on the CONSEQ server prediction. A hepta-oligoribonucleotide (5'-A-U-U-U-U-G-3') with end terminals capped was used for simulation. The summary for the different model systems is listed in Table 1. In each system the charge of the protein was neutralized by adding Na⁺ or Cl⁻ ions modulated by AMBER99 and systems were finally solvated with approximately 20500 TIP3P water molecules.

2.4. Mutant protein stability prediction using CUPSAT server

The protein stability for each point mutation on the Hfq protein was predicted using CUPSAT prediction server (<http://cupsat.tu-bs.de/>) [30]. This tool predicts the changes in protein stability upon the point mutations. The prediction model uses amino acid-atom potentials and torsion angle distribution to assess the amino acid environment of the mutation site. Additionally, the prediction model can distinguish the amino acid environment using its

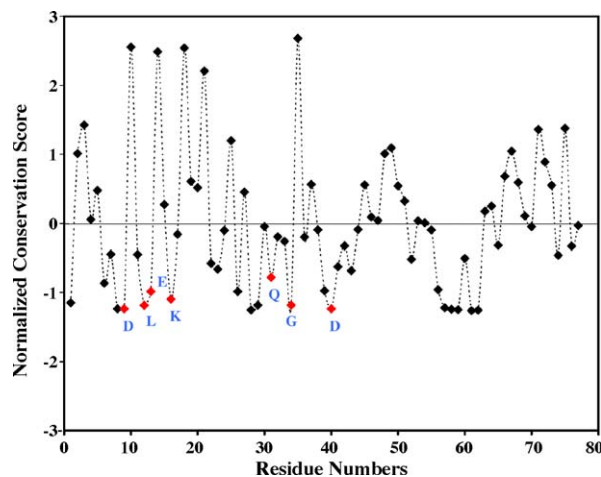


Fig. 4. Degree of conservation scores for each residue in Hfq protein sequence. The seven residues are labeled.

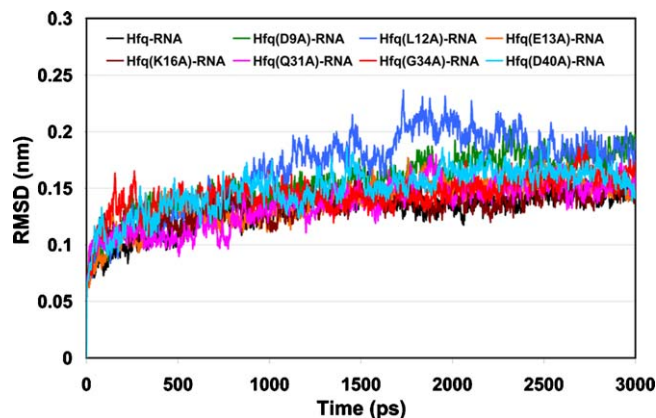


Fig. 5. Time dependence of the root mean square deviation (RMSD) for the protein backbone atoms during the simulation in Hfq-RNA complexes of all the systems.

solvent accessibility and secondary structure specificity. It uses protein environment specific mean force potentials to predict the protein stability. In case of unfavorable torsion angles, the atom potentials may have higher impact on the stability of Hfq–RNA complex which results in destabilizing the system. The CUPSAT server includes the overall stability change calculated using the atom and torsion angle potentials together, the adaptation (favorable or unfavorable) of the observed torsion angle combination and the predicted $\Delta\Delta G$. The negative and positive predicted $\Delta\Delta G$ values mean the destabilizing and stabilizing effect, respectively. Overall stability of the Hfq mutants bound with

RNA is calculated based on atom potentials and torsion angle potentials. The predicted stability energy ($\Delta\Delta G$) values for each of the point mutant systems were analyzed separately.

3. Results and discussions

3.1. Prediction of structurally and functionally important residues located distant from NBP using CONSEQ server

The *S. aureus* Hfq sequence was analyzed using the CONSEQ server which predicted the highly conserved and exposed

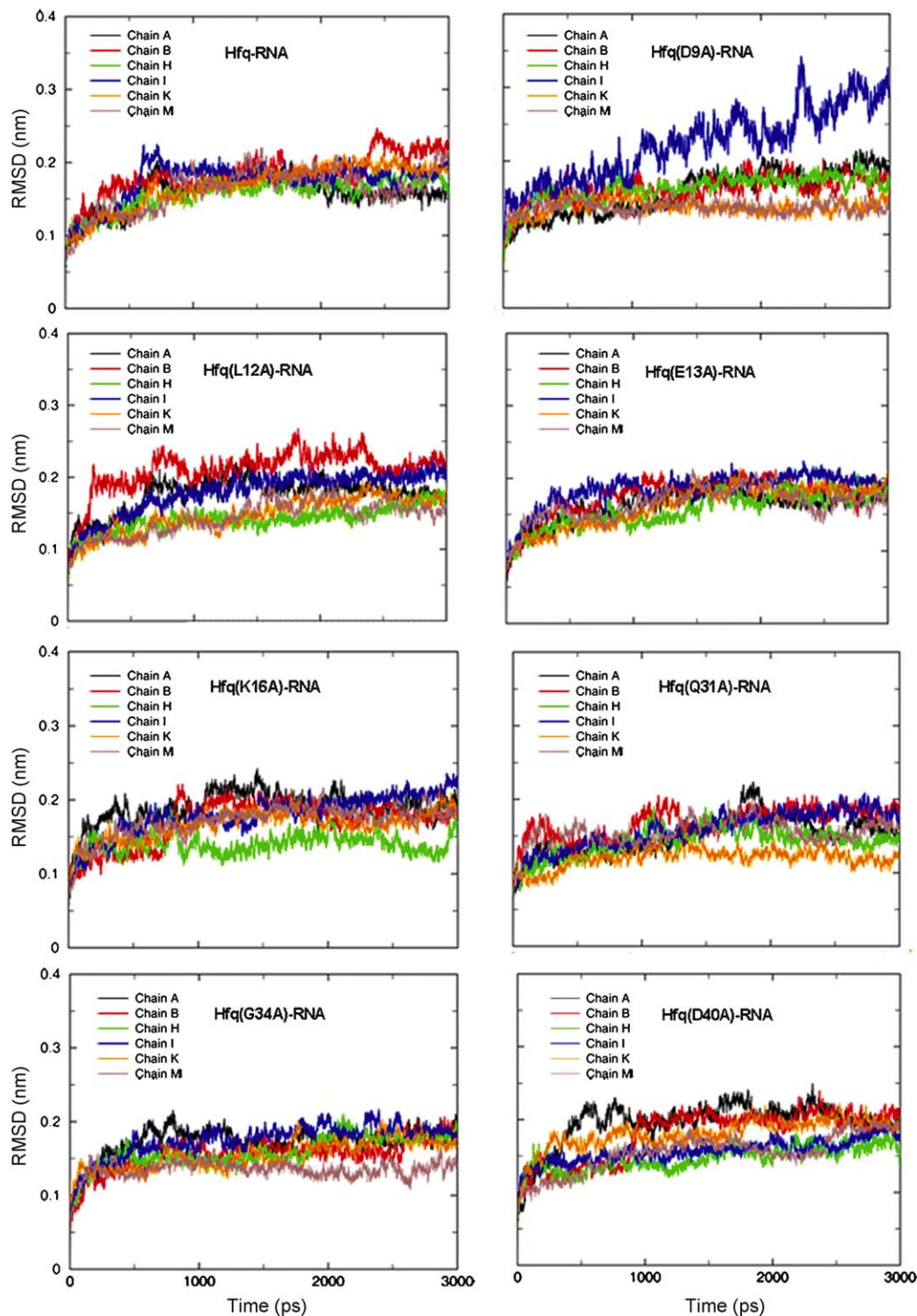


Fig. 6. Time dependence of the RMSD for the backbone atoms of each monomer (chain) of the Hfq hexamer during the simulation for all the complex systems.

functional and buried structural residues for the given sequence. Based on the result, the seven residues Asp9, Leu12, Glu13, Lys16, Gln31, Gly34 and Asp40 were selected and then considered for mutation and MD simulation study (Figs. 2 and 3). It so happens that these seven residues are not directly involved in the RNA binding because they are located far from the NBP. Nonetheless the seven residues predicted to be functionally and structurally important by the CONSEQ server. This is very interesting result to us and hence the mutation study was carried out. However, their role in the influence of the RNA binding to the Hfq protein remains unclear until now.

In order to estimate the degrees of conservation of each residue the normalized conservation score of the residues of protein were calculated (Fig. 4). The negative and positive deviations represent the conservations and variations, respectively. The result shows that the seven residues are strongly conserved in the protein. Most of the highly conserved functional and structural residues far and near to the nucleotide-binding portion have negative deviations. Many of the structurally and functionally important residues are directly involved in the nucleotide-binding mechanism.

3.2. MD simulation studies for the model systems

MD simulations were performed to (i) study the conformational changes taking place in Hfq with bound RNA and (ii) to investigate the importance of the seven residues located far from NBP of Hfq. During simulation, the RMSD and RMSF of the individual monomers, bases and protein backbone of the systems were monitored. The RMSD values versus simulation time of all the Hfq systems were increased gradually until first 1 ns. After this time, the values of the Hfq–RNA complex and mutant complexes E13A, K16A, Q31Q, G34A and D40A were stabilized, whereas the values of the mutant complexes D9A and L12A continued to gradually increase and reached a stable level after nearly 2 ns. The mutants L12A and D9A showed little more deviation than the other systems (Fig. 5). The stability of each chain (monomer) of the Hfq hexamer movements were also observed separately and it was found that during the simulation the chain I deviated considerably after 1 ns in the mutant D9A and also in mutant L12A the chains B and I deviated significantly (Fig. 6). It seems that these differences explain the overall RMSD difference for mutants D9A and L12A in Hfq bound RNA compared to native complex and other mutants in Fig. 5.

The average residue fluctuations of the proteins were observed by calculating root mean square fluctuation (RMSF). Each mutant system individual residue fluctuations were compared to the wild-type Hfq–RNA complex residue fluctuations (Fig. 7). Not much difference was found in the residue fluctuation and only minor displacement was found in D9A and L12A mutants. We also noticed a considerable change in the chain I and K residues of the mutants. In general only the variable loop region residues undergo a displacement more than 0.2 nm. It is noted that most mutants restrain the fluctuation of chain K residues especially Asn28. The Asn28 is highly conserved functionally important residue, which reads the hydrogen bond donors and acceptors of the adenine ring together with Gln52 [18]. The functional and structural importance of this chain K and Asn28 residue in particular is unknown yet. Our analysis reveals that some residue mutations can influence the movement of that particular residue.

The movement of bases of the RNA nucleotides was also monitored during the simulation time (Fig. 8). The wild-type Hfq and mutants D9A, E13A and K16A had major movement in the bases comparing to its original position. The deviation of Guanine base is obvious as it is the only residue that was found hanging in the middle of the Hfq pore, all other bases are well stacked between aromatic side chains of Tyr42 residue of neighboring subunits/monomers. Our study shows clearly that in mutations D9A, E13A

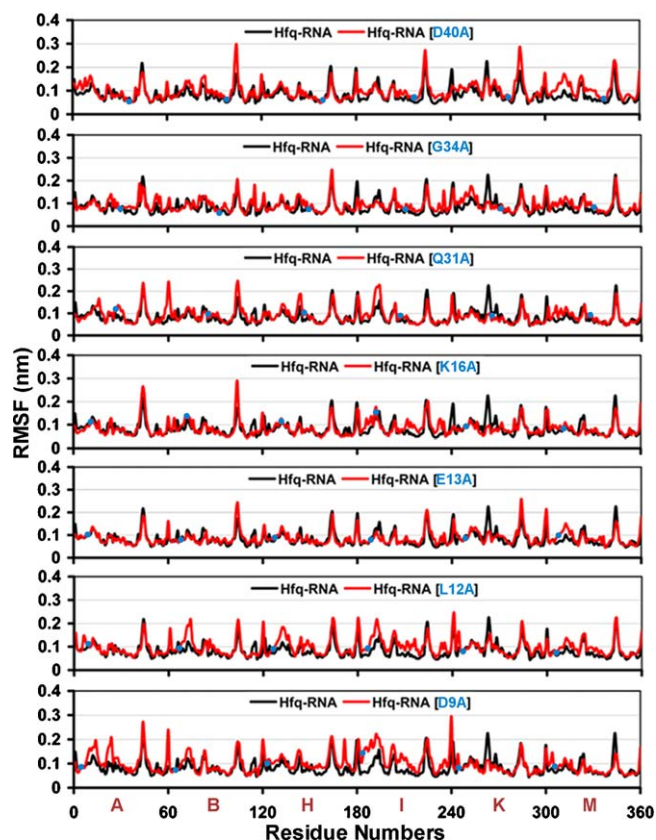


Fig. 7. The root mean square fluctuation (RMSF) with respect to each residue of the Hfq protein during the simulation for all the mutant systems with reference to the wild-type complex. Blue dots represent the exact position of each specific hexamutants.

and K16A the base stacking have been greatly affected, which may be due to the influence of mutation on the base stacking residue Tyr42 of the monomers whose aromatic side chain has moved from its original position, which provided the stacking atmosphere for the adenine and uridine nucleobases. This led to the conclusion that the mutants D9A, E13A and K16A may have an influence on the base stacking, although the residue mutated were located far from the NBP. The Hfq pore diameter was also examined since a specific pore diameter is required for the threading of RNA through the pore for the post-translational modification (Table 2). The pore diameter was calculated by measuring the distance from the center of atom of one of the pore lining residue from the highly conserved YKHAI motif of one chain to the exactly opposite chain and the same pore lining residue. Here we have used residue His58 of the YKHAI motif of chain A and the exactly opposite chain K to calculate the pore diameter. The arrangements of chains in *S. aureus* Hfq are shown in Fig. 1. The pore diameter of the wild-type Hfq–RNA complex is between 1.2 and 1.4 nm, but we found that the pore diameter increased to about 1.7 nm in the mutants L12A and E13A during the simulation. Hence it is inferred that the mutants L12A and E13A may enhance or weaken the post-translational modification, more specifically the assembly/remodeling of RNA–protein complexes and hence threading of RNA through the pore.

3.3. Prediction of protein mutant stability using CUPSAT server

We studied the effect of each point mutation on the Hfq protein by the CUPSAT server. Destabilization of the Hfq–RNA complex was observed probably due to the unfavorable torsion angles, and the atom potentials. Hence the overall stability of the Hfq mutants

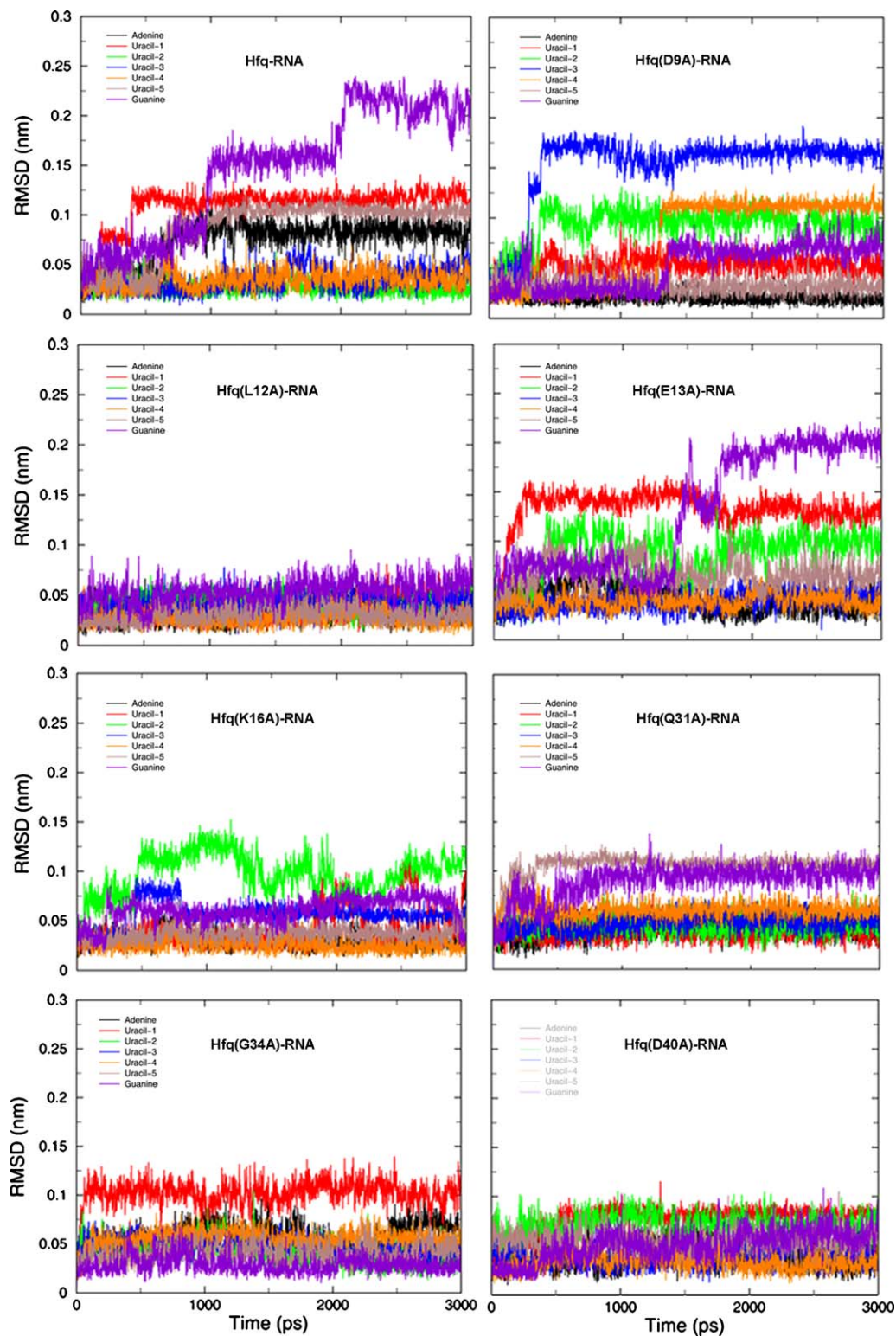


Fig. 8. Time dependence of the RMSD of each base of the ribonucleotide (AU₅G) bound to Hfq during the simulation for all the systems.

bound with RNA is calculated based on atom potentials and torsion angle potentials. The result revealed that most mutants, except for Q31A were destabilized by the mutation effect. The predicted destabilizing energy ($\Delta\Delta G$) values show that the mutants G34A (-3.93 kcal/mol), L12A (-2.11 kcal/mol), E13A (-1.23 kcal/mol) and D9A (-1.21 kcal/mol) have significant influence on Hfq by the point mutation (Table 3). According to CUPSAT server, a negative

$\Delta\Delta G$ value is indicative of protein destabilization which is predicted based on the stability changes in protein upon point mutation accurately by measuring the free energy difference between folded and unfolded state $\Delta\Delta G$. This can be translated, as those residues are very important for the protein to function and may play a role in the RNA binding and assembly/remodeling of RNA–protein complexes.

Table 2

Hfq pore diameter for all the systems averaged over the last 2 ns in the simulation time.

No.	System details	Average pore diameter (nm)
1	Hfq + RNA	1.28
2	Hfq(D9A) + RNA	1.42
3	Hfq(L12A) + RNA	1.69
4	Hfq(E13A) + RNA	1.57
5	Hfq(K16A) + RNA	1.45
6	Hfq(Q31A) + RNA	1.52
7	Hfq(G34A) + RNA	1.56
8	Hfq(D40A) + RNA	1.45

Table 3

Predicted protein destability for all the seven point mutations (hexamutants) analyzed by the CUPSAT server.

Mutant	Overall Stability	Torsion	Predicted $\Delta\Delta G$ (kcal/mol)
D9A	Destabilizing	Favorable	-1.21
L12A	Destabilizing	Favorable	-2.11
E13A	Destabilizing	Unfavorable	-1.23
K16A	Destabilizing	Favorable	-0.28
Q31A	Stabilizing	Unfavorable	0.51
G34A	Destabilizing	Unfavorable	-3.93
D40A	Destabilizing	Unfavorable	-0.47

Table 4

Interaction energies calculated between Hfq and RNA of the complexes for all the systems.

No.	System details	Interaction energy ^a (kcal/mol)	van der Waals energy (kcal/mol)
1	Hfq + RNA	-590.8	-173.3
2	Hfq(D9A) + RNA	-544.4	-156.0
3	Hfq(L12A) + RNA	-646.7	-166.1
4	Hfq(E13A) + RNA	-519.6	-138.3
5	Hfq(K16A) + RNA	-578.4	-161.9
6	Hfq(Q31A) + RNA	-589.9	-163.9
7	Hfq(G34A) + RNA	-611.6	-154.8
8	Hfq(D40A) + RNA	-575.9	-143.0

^a Sum of van der Waals energy and electrostatic interaction energy. The values of electrostatic interaction energies are not shown.

3.4. Analysis of interaction energy in the Hfq–RNA complexes

The interaction energies between the mutant Hfq and RNA complexes were also examined with the conformation which is most similar to the averaged structure during the simulation time. It is noted that the most favorable or strong interaction was found in L12A mutant whereas the E13A mutant showed the weakest interaction. Those differences were mostly due to differences in the van der Waals interaction energy between Hfq and RNA (Table 4). This indicates that these two mutations cause most significant changes compared to the native or wild-type form and other mutants. This result suggests that the residues Leu12 and Gln13 should be conserved as the native form for the protein function and furthermore that the both residues may play an important role on the assembly/remodeling of RNA–protein complexes.

Through nine MD simulations and the CONSEQ/CUPSAT analyses we substantiate the seven residues effect on RNA binding and reveal residues Asp9, Leu12, Gln13 and Gly34 located far from the NBP which may have an effect on Hfq mechanism.

4. Conclusions

Our objective of this study was to uncover some important residues which are located far from the NBP but may have a

conformational and functional effect on Hfq mechanism. In order to achieve the goal, at first the CONSEQ server analysis was performed for the *S. aureus* Hfq sequence to find the structurally buried and functionally exposed important residues and finally the seven residues were selected. The seven residues selected for our study have high conservation scores based on evolutionary relationship among the family of homologs, and they are all predicted to have structural and/or functional importance for the protein by the server. There may be other residues whose mutations may have similar effect. But our intention was to target only those residues that are far from the NBP and are functionally and structurally important residues of Hfq. Hence we have chosen all the residues that are far from the NBP and are predicted to be functionally and structurally important based on the conservation scores. And then nine MD simulations were introduced for the wild-type and the seven mutants which were constructed by the point mutation at the seven residues (every single mutant here is a hexamutant) in order to investigate the residue and mutation effect for those seven residues. The results revealed the crucial role of the mutants D9A, E13A and K16A on the base stacking by disrupting the aromatic stacking of the Tyr42 residue of the adjacent subunits/monomers and on the increase in RNA pore diameter in mutants L12A and E13A, which is required for the threading of single stranded RNA through the pore for the post-translational modification.

Also the Asn28 which is an already known functionally important residue of Hfq was observed to be the most dynamically stable residue in chain K from all the mutants. Furthermore, the protein stability change caused by the point mutations was observed by the CUPSAT server analysis. The results showed destabilization effect for the most mutants except for Q31A. The destabilization value was observed to be high in the mutants D9A, L12A, E13A and G34A. This suggests that the residues Asp9, Leu12, Gln13 and Gly34 located distant from the NBP may be important for Hfq function and mechanism in *S. aureus* Hfq.

The interaction energies observed between the mutant Hfq and RNA complexes showed most favorable or strong interaction in L12A mutant and a weak interaction scenario in the E13A mutant. It means that these two mutations probably have significant effect on the Hfq–RNA complex compared to the native form and other mutants. Our study and the corresponding result suggest the importance of the residues Leu12 and Gln13 to be well conserved in the native form for the protein function and furthermore that the both residues may play an important role on the assembly/remodeling of RNA–protein complexes. Hence our study reveals that, few mutations affect the RNA interaction with the Hfq protein and some affect the overall stability of the protein. Additional in vivo analysis is essential for the confirmation of the mutant effect on the Hfq protein function and mechanism.

In conclusion, this study provides a direction to proceed in analyzing the structure function relationship of the important sRNA- and mRNA-binding proteins focusing on some of the key residues far from the NBP of Hfq apart from the already known residues.

Acknowledgments

Prettina Lazar, Songmi Kim, Yuno Lee and Minky Son are recipients of fellowship from the BK21 Programs and this work was supported by grants from the MOST/KOSEF for the Environmental Biotechnology National Core Research Center (grant #R15-2003-012-02001-0)

References

- [1] M.T. Franze de Fernandez, L. Eoyang, J.T. August, Factor fraction required for the synthesis of bacteriophage Qbeta-RNA, *Nature* 219 (154) (1968) 588–590.

- [2] Y. Ding, B.M. Davis, M.K. Waldor, Hfq is essential for *Vibrio cholerae* virulence and downregulates sigma expression, *Mol. Microbiol.* 53 (1) (2004) 345–354.
- [3] G.T. Robertson, R.M. Roop Jr., The *Brucella abortus* host factor 1 (HF-1) protein contributes to stress resistance during stationary phase and is a major determinant of virulence in mice, *Mol. Microbiol.* 34 (4) (1999) 690–700.
- [4] H. Nakao, H. Watanabe, S. Nakayama, T. Takeda, yst gene expression in *Yersinia enterocolitica* is positively regulated by a chromosomal region that is highly homologous to *Escherichia coli* host factor 1 gene (*hfq*), *Mol. Microbiol.* 18 (5) (1995) 859–865.
- [5] E. Sonnleitner, S. Hagens, F. Rosenau, S. Wilhelm, A. Habel, K.E. Jager, U. Blasi, Reduced virulence of a *hfq* mutant of *Pseudomonas aeruginosa* O1, *Microb. Pathog.* 35 (5) (2003) 217–228.
- [6] N. Figueroa-Bossi, S. Lemire, D. Maloriol, R. Balbontin, J. Casadesus, L. Bossi, Loss of Hfq activates the sigma-dependent envelope stress response in *Salmonella enterica*, *Mol. Microbiol.* 62 (3) (2006) 838–852.
- [7] A.K. Sharma, S.M. Payne, Induction of expression of *hfq* by DksA is essential for *Shigella flexneri* virulence, *Mol. Microbiol.* 62 (2) (2006) 469–479.
- [8] A. Sittka, V. Pfeiffer, K. Tedin, J. Vogel, The RNA chaperone Hfq is essential for the virulence of *Salmonella typhimurium*, *Mol. Microbiol.* 63 (1) (2007) 193–217.
- [9] J.K. Christiansen, M.H. Larsen, H. Ingmer, L. Sogaard-Andersen, B.H. Kallipolitis, The RNA-binding protein Hfq of *Listeria monocytogenes*: role in stress tolerance and virulence, *J. Bacteriol.* 186 (11) (2004) 3355–3362.
- [10] P. Valentin-Hansen, M. Eriksen, C. Udesen, The bacterial Sm-like protein Hfq: a key player in RNA transactions, *Mol. Microbiol.* 51 (6) (2004) 1525–1533.
- [11] A. Zhang, K.M. Wassarman, C. Rosenow, B.C. Tjaden, G. Storz, S. Gottesman, Global analysis of small RNA and mRNA targets of Hfq, *Mol. Microbiol.* 50 (4) (2003) 1111–1124.
- [12] X. Sun, I. Zhulin, R.M. Wartell, Predicted structure and phyletic distribution of the RNA-binding protein Hfq, *Nucleic Acids Res.* 30 (17) (2002) 3662–3671.
- [13] M. Höök, T.J. Foster, *Staphylococcal Surface Proteins*, ASM Press, Washington, 2000.
- [14] R.P. Novick, Autoinduction and signal transduction in the regulation of staphylococcal virulence, *Mol. Microbiol.* 48 (6) (2003) 1429–1449.
- [15] M.A. Schumacher, R.F. Pearson, T. Moller, P. Valentin-Hansen, R.G. Brennan, Structures of the pleiotropic translational regulator Hfq and an Hfq–RNA complex: a bacterial Sm-like protein, *Embo J.* 21 (13) (2002) 3546–3556.
- [16] P. Valentin-Hansen, M. Eriksen, C. Udesen, The bacterial Sm-like protein Hfq: a key player in RNA transactions, *Mol. Microbiol.* 51 (2004) 1525–1533.
- [17] G. Storz, J.A. Opdyke, A. Zhang, Controlling mRNA stability and translation with small, noncoding RNAs, *Curr. Opin. Microbiol.* 7 (2004) 140–144.
- [18] R.G. Brennan, T.M. Link, Hfq structure, function and ligand binding, *Curr. Opin. Microbiol.* 10 (2007) 1–9.
- [19] K. Ziolkowska, P. Derreumaux, M. Folichon, O. Pellegrini, P. Regnier, I.V. Boni, E. Hajnsdorf, Hfq variant with altered RNA binding functions, *Nucleic Acids Res.* 34 (2006) 709–720.
- [20] C. Berezin, F. Glaser, Y. Rosenberg, I. Paz, T. Pupko, P. Fariselli, R. Casadio, N. Ben-Tal, ConSeq: the identification of functionally and structurally important residues in protein sequences, *Bioinformatics* 20 (2004) 322–3324.
- [21] H.J.C. Berendsen, D. van der Spoel, R. van Drunen, GROMACS: a message-passing parallel molecular dynamics implementation, *Comp. Phys. Commun.* 91 (1995) 43–56.
- [22] E. Lindahl, B. Hess, D. Van der Spoel, GROMACS 3.0: a package for molecular simulation and trajectory analysis, *J. Mol. Mod.* 7 (2001) 306–317.
- [23] J. Eric Sorin, S. Vijay Pande, Exploring the helix-coil transition via all-atom equilibrium ensemble simulations, *Biophys. J.* 88 (4) (2005) 2472–2493.
- [24] W.L. Jorgensen, J. Chandrasekhar, J.D. Madura, R.W. Impey, M.L. Klein, Comparison of simple potential functions for simulating liquid water, *J. Chem. Phys.* 79 (1983) 926.
- [25] U. Essman, L. Perela, M.L. Berkowitz, T. Darden, H. Lee, L.G. Pedersen, A smooth particle mesh Ewald method, *J. Chem. Phys.* 103 (1995) 8577–8592.
- [26] H.J.C. Berendsen, J.P.M. Postma, A. Di Nola, J.R. Haak, Molecular dynamics with coupling to an external bath, *J. Chem. Phys.* 81 (1984) 3684–3690.
- [27] M. Parrinello, A. Rahman, Polymorphic transition in single crystals: a new molecular dynamics method, *J. Appl. Phys.* 52 (1981) 7182–7190.
- [28] B. Hess, H. Bekker, H.J.C. Berendsen, J.G.E.M. Fraaije, LINCS: a linear constraint solver for molecular simulations, *J. Comp. Chem.* 18 (1997) 1463–1472.
- [29] J.P. Ryckaert, G. Ciccotti, H.J.C. Berendsen, Numerical integration of the Cartesian equations of motion of a system with constraints: molecular dynamics of n-alkanes, *J. Comp. Phys.* 23 (1977) 327–341.
- [30] V. Parthiban, M.M. Gromiha, D. Schomburg, CUPSAT: prediction of protein stability upon point mutations, *Nucleic Acids Res.* 34 (2006) 239–242.